Metering Performance Investigation and Substantiation of the "Universal Venturi Tube" (U.V.T.)

The UVT provides Classical Venturi tube type metering performance with less than half the laying length, no annular chambers, and about half the permanent head loss. Data presented reveal the flow mechanism inside the tube and substantiate its performance over a wide range of Reynolds numbers, line sizes, beta ratios, tube materials, upstream and downstream piping configurations for incompressible and compressible flow. The experience of the past five years indicates ± 0.5 percent two times standard deviation uncalibrated accuracy for C.I. UVT's. Due to its depth and method, the substantiation work was unique; consequently, it is recommended as a standard procedure for the performance substantiation of any kind of flow meter presently in use or to be introduced in the future.

Part 1—Hydraulic Shape and Discharge Coefficient

Introduction

About 20 years ago, a group of "modified Venturi tubes" were introduced in flow metering having the following common characteristics: [2–5][1]

- Extremely short laying length (less than half that of the short form Classical Venturis)
- Drastic magnification of the differential pressure signal (about twice that of the Classical Venturis)
- Low permanent head loss, especially when expressed in percent of this magnified differential (one-third to one-half that of the Classical Venturis at higher beta ratios).

The family of these devices was identified as "Flow Tubes" and soon practically eliminated the Classical Venturi tubes from common usage. The sudden success is understandable due to the above-mentioned unquestionable features and the following performance claims:

- ±1 percent uncalibrated accuracy
- Constancy of C at high R_D's
- Normal installation effect.

While more thorough investigations [3, 4] indicated already at the outset that Flow Tubes are much more sensitive to certain installation effects than Classical Venturi tubes, to prove the validity of the rest of the claim required substantial time. Why? Because to establish the uncalibrated accuracy of any device requires sizable data accumulation and its statistical analysis, and to check C behvaior at high R_D's requires adequate calibrating capacity which, for a time, was not available.

Since the past 20 years provided numerous calibration data and recently a hydraulic lab (Alden Research Lab) became available capable of running calibrations accurately to high R_D's, the following facts became evident.

[1]Numbers in brackets designate References at end of paper.

Contributed by the Research Committee on Fluid Meters for presentation at the Winter Annual Meeting, Detroit, Mich., November 11-15, 1973, of The American Society of Mechanical Engineers. Manuscript received at ASME Headquarters, July 23, 1973. Paper No. 73-WA/FM-3.

Copies will be available until August, 1974.

First. As Fig. 1 shows, the uncalibrated accuracy [1] of Dall tubes was found to be ±3.32 percent when calculated by a strict two times standard deviation process [2] based on data collected for 20 years with no data discarded. It must be noted, however, that this value refers to 0.4 to 0.8 beta ratio tubes, and the twice standard deviation is smaller for the smaller beta ratios and larger for the larger beta ratio ones.

Second. Fig. 2 shows the C behavior from an R_D of 0.2×10^6 to 4×10^6 for a 21.225-in. Dall tube. (To reach such high R_D's became possible only recently at Alden Research Lab's new calibration facility where 100,000 lb of water can be heated to temperatures well over ambient.) The data contradicted previous beliefs—that the C stays constant at higher R_D's, making the use of Flow Tubes for high R_D metering questionable.

Spot-checks performed by author's company indicated similar difficulties with other types of commonly used Flow Tubes; while the following warning in *ASME Fluid Meters*, 6th edition,

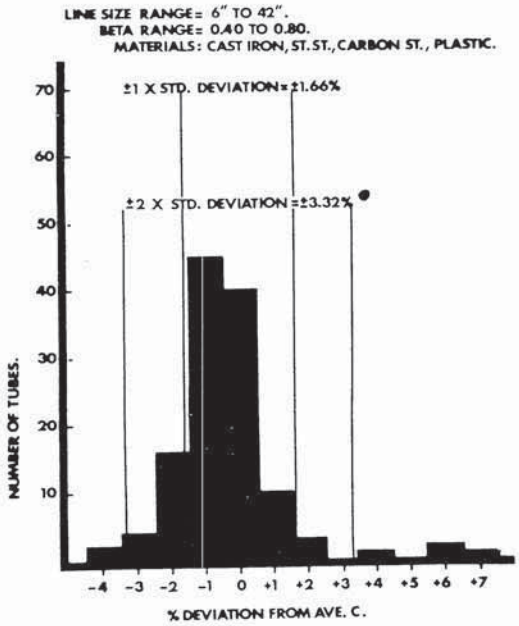

Fig. 1 Calibrated mean C deviations from the standard value for dall tubes

1971, Paragraph II–III–48 substantiates that the problem is general:

"If one of these Flow Tubes is to be used, it should be calibrated with the piping section in which it is to be used and over the full range of rates of flow to which it will be subjected when in use."

The foregoing facts revealed an obligation which, in view of the wealth of already available performance data, became an intriguing task: namely, to design a tube that unites (hence the designation Universal Venturi tube) the desirable characteristics of all known differential producers, i.e.:

- The C value is high.
- The C is constant from low R_D's up to the highest ones.
- The C is independent of beta ratio.
- The C is not influenced by line size.
- The C is influenced only slightly by flow pattern changes.
- The uncalibrated C accuracy is high due to the insensitivity of the tube hydraulic shape to large manufacturing tolerances [2].
- The C value, behavior, and uncalibrated accuracy level ($2 \times$ standard deviation) can be predicted by reliable semiempirical calculations.
- The C is unaffected by downstream piping.
- The adiabatic expansion factor can be calculated.
- The differential is "quiet."
- The laying length is short.
- The permanent head loss is low.

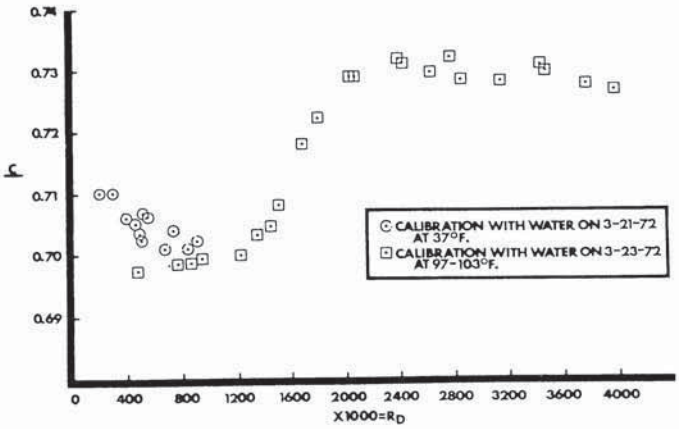

Fig. 2 Calibration of a 21.255 in. X 12.066 in., beta = 0.5677, dall tube

The author's company began the development of such a device five years ago; consequently, this paper is a report of the more important findings of the development work as well as of the experience obtained during this time period with the device.

1 The Hydraulic Shape

The final hydraulic shape selected for the U.V.T. is shown in Fig. 3. All performance data presented in the paper were obtained on this shape which has the following salient characteristics:

1.1 Transition Section. The transition section (Fig. 3(*a*)) is composed of a 40-deg inlet and a 7-deg throat cone (half angle) with no smooth blending radii at the lines of intersection.

The axial wall pressure profile in such transition sections with different inlet cone angles can be seen in Figs. 4, 5, 6, and 7. On these figures, results of tests are shown which were conducted at BIF's Hydraulic Lab with water as line fluid, on a 6×4.499-in., 0.7498 beta and a 6×1.903-in., 0.3172 beta bronze models. Numerous holes, with axis perpendicular to the tube axis, were located in these models facilitating the exploration of the flow mechanism.

These tests indicated the following characteristics:

(*A*) The transition section caused flow separations (vena contractae) at the intersection of the inlet and throat cone and of the throat cone and the throat section. The location of these vena contractae were verified by observing in a 6-in. 0.4 beta plexiglass tube the cross section where incipient cavitation set in. These cross sections coincided with the intersection lines.

(*B*) In all cases these vena contractae reattached to the throat cone wall, or to the cylindrical throat wall within a distance of about $^1/_4$ of the local diameter. This fact was verified again by the aforementioned transparent tube tests, because the discoloration, indicating incipient cavitation, disappeared as the flow moved out of the cross section of the vena contractae.

(*C*) Wall pressures near to and downstream from the vena contractae fluctuated more than in regions of reattached flow.

(*D*) The location of the vena contractae stayed in the same place as R_D was changed.

1.2 Entrance Section. In the entrance section, indicated by M in Fig. 3(*a*) the wall pressure rises (Figs. 4, 5, 6, and 7) and reaches its maximum value in the corner formed by the intersection of the entrance section and inlet cone.

This wall pressure rise is caused by a change in the direction of the local flow brought about by the inlet cone. Its magnitude is about a constant portion of the inlet velocity head; thus, its effect on a differential measured between the inlet corner tap and the throat tap becomes a function of beta and diminishes as beta decreases.

Distance M for U.V.T.'s is a function of beta locating the inlet tap at a point where the rise of the grade line just begins to become noticeable, thus tying it hydraulically to the tube.

1.3 Throat Section. The length of the cylindrical throat is $d/2$ (Fig. 3(*a*)) with no blending radii at its entrance and exit.

The investigation performed to explore the flow mechanism in the throat revealed as follows:

(*A*) The wall pressure lines indicate (Figs. 4, 5, 6, 7, and 8) flow separations at the entrance as well as at the exit of the cylindrical throat.

The fact that vena contactae are formed at those intersection lines was proven by the incipient cavitation lines observed in the 6-in. transparent tube which disappeared as the flow moved out of these cross sections.

(*B*) The location of these vena contractae is independent of R_D.

(*C*) According to the evidence of Fig. 8, the downstream vena contracta caused the wall pressure rise in wall taps located in the upstream half of the throat section as the throat length was shortened.

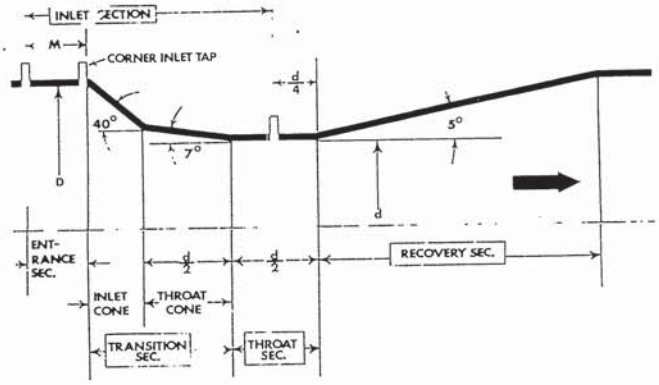

Fig. 3(*a*) The hydraulic shape of the U.V.T.

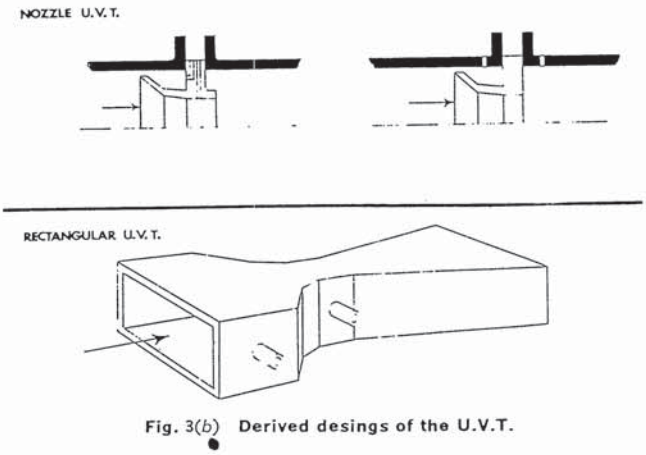

Fig. 3(*b*) Derived desings of the U.V.T.

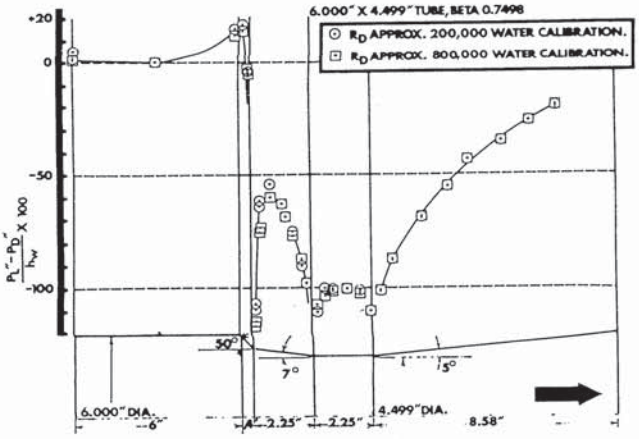

Fig. 4 Axial wall pressure profile

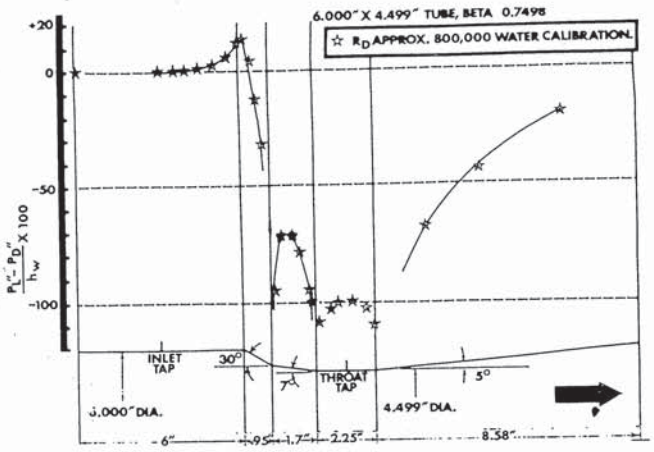

Fig. 5 Axial wall pressure profile

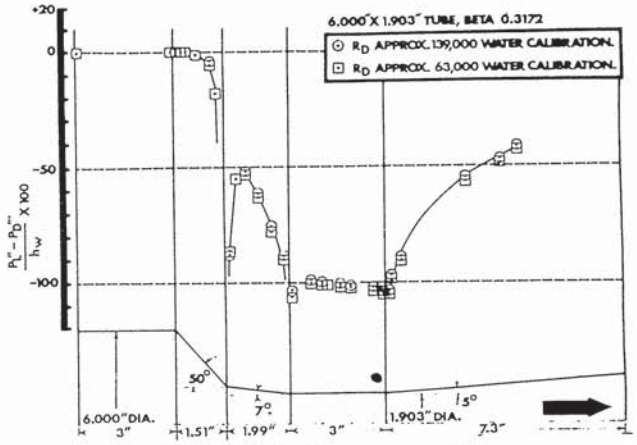

Fig. 6 Axial wall pressure profile

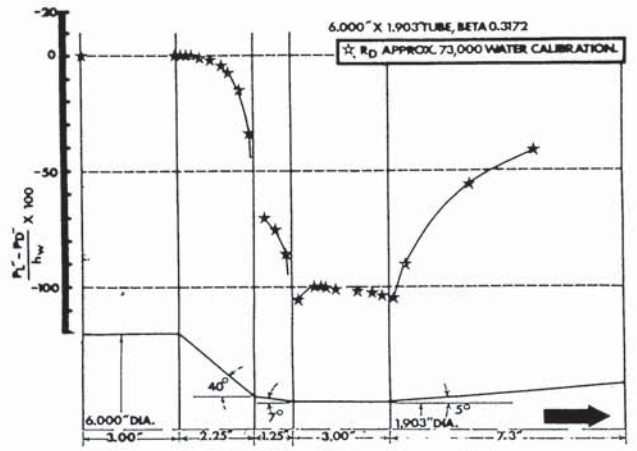

Fig. 7 Axial wall pressure profile

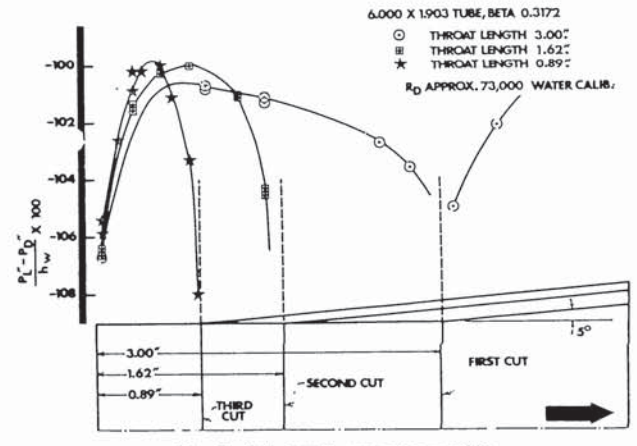

Fig. 8 Axial wall pressure profile

(*D*) The wall pressure line became symmetrical in the upstream and downstream half of the throat for throat length equal to $d/2$, indicating reattached flow at the throat tap cross section which fact was proven by the transparent tests also.

(*E*) Fig. 9 shows the velocity profiles found in the 6-in., 0.7498 beta model.

The alpha values indicate the ratios of the actual kinetic energy content to the ideal one at different tube cross sections at 700,000 R_D. It is interesting to note that the 1.041 alpha value at the inlet tap cross section decreased to 1.003 in the throat due to the hydraulic shape of the transition section, approaching well the ideal value of 1.

Furthermore, the velocity profiles were found to be similar at the inlet, outlet, and middle cross sections of the throat, indicating that the blunt flow pattern develops near to the throat entrance and stays so throughout its length.

1.4 Recovery Section. The recovery cone included cone angle was selected to be 10 deg (Fig. 3(*a*)) for all beta ratios with no smooth blending radii at the throat to recovery cone intersection line.

The investigation revealed the following flow mechanism:

(*A*) Figs. 4, 5, 6, 7 indicate that the wall pressure rises suddenly right after the cone entrance cross section, promising efficient conversion of the kinetic head into static pressure, while

(*B*) Fig. 9 shows velocity profiles measured in the recovery cone near to its entrance and exit cross sections, the latter indicating no flow separation.

The data presented so far show the method used to explore the basic flow mechanism in the U.V.T. hydraulic shape as well as the most important and/or typical findings.

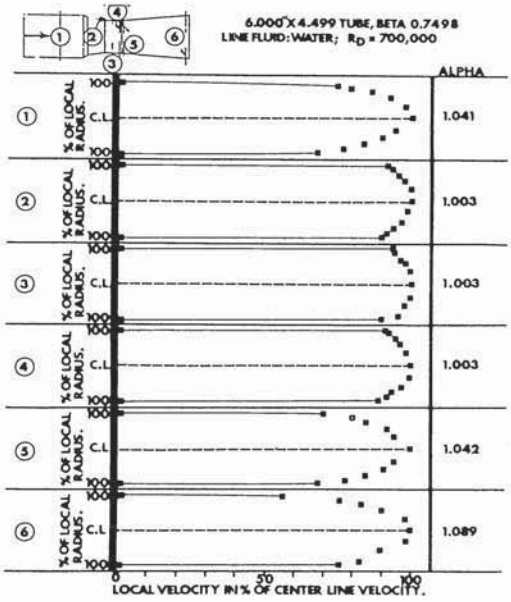

Fig. 9 Velocity profiles

Next the performance test data shall be presented obtained on U.V.T.'s having the hydraulic shape as shown in Fig. 3(*a*).

To save space, the testing facilities shall not be described in detail unless proper data interpretation requires it. It should be stated, however, that all tests were performed in recognized hydraulic labs by people experienced in this type of work.

It should be emphasized furthermore that most installation effect tests were run by using the standard U.V.T. static inlet tap and a corner inlet tap located adjacent to the inlet cone [Fig. 3(*a*)] simultaneously with the purpose of obtaining a better understanding on how *C* deviations are composed—to check the test work and to collect data for corner tapped U.V.T. applications.

2 *C* of the UVT

2.1 The Value and Beta Dependence of *C*. Up until the time of writing this paper, 51 standard U.V.T.'s had been calibrated with water, some at Alden Research Lab and some at BIF Hydraulic Lab. These calibrations included tubes 3 to 42-in. line sizes, with beta ratios between 0.20 and 0.75, made of various materials (stainless and carbon steel, cast iron, plastic, plexiglass) and with different extents of machining; namely, no tube had machined entrance section, some had fully machined transition and throat section; while only the throat or throat and throat cone were machined for others. Fig. 11 shows a

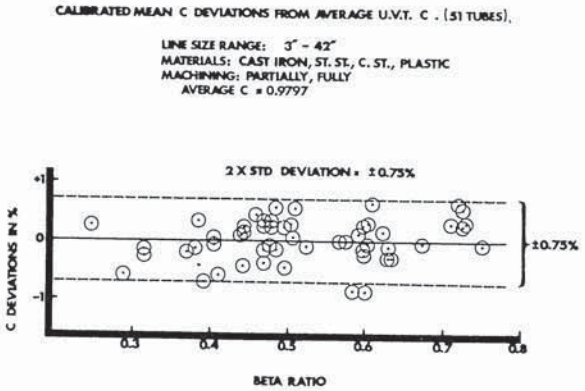

Fig. 10 Beat ratio effect on *C*

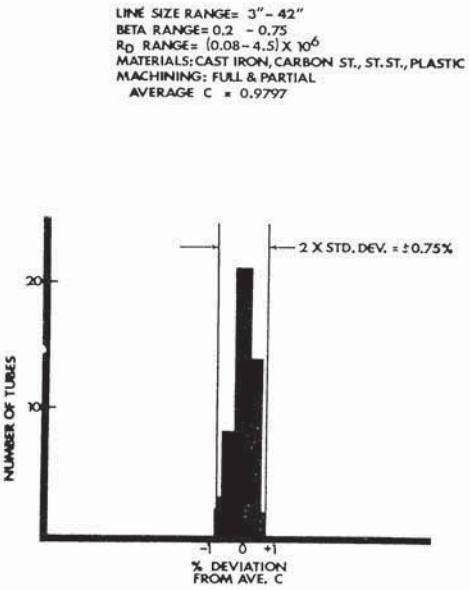

Fig. 11 Calibrated mean *C* data for 51 standard U.V.T.'s (600 calibration points)

0.9797 average *C* value for these tubes, as well as the distribution of the calibrated mean *C* deviations from this average *C* value in percent.

The same data is replotted in Fig. 10 in the function of beta ratio to show that the 0.9797 U.V.T. standard *C* is independent of beta ratio within the 2 × standard deviation tolerance band. (Further verification can be found in Fig. 13 for the cast iron portion of the 51 U.V.T.'s.)

Above *C* behavior proves that the inlet and throat taps "see" true static pressures, further supporting the findings of the wall pressure tests (Figs. 4, 5, 6, and 7).

The important consequence of this fact is that the *C* value and behavior of the U.V.T. can be predicted by reliable semi-empirical calculations based on the following formula developed for Classical Venturi tubes (reference [7]).

$$C = \sqrt{\frac{1 - \beta^4}{\alpha d - \alpha D \beta^4 + H_L}} \qquad (1)$$

In equation (1), α_d and α_D are kinetic energy factors at the throat and inlet cross sections, respectively, which approach the value of 1 above a certain R_D; consequently, over that R_D, they cannot cause C beta sensitivity.

H_L is the head loss factor defining the energy loss in terms of throat velocity head, occurring in the tube between the inlet and throat tap cross sections.

H_L values calculated from equation (1) for the standard U.V.T. C value of 0.9797 are shown in Fig. 12. As illustrated H_L must decrease with increasing beta to provide the beta insensitivity observed with U.V.T.'s which is the characteristic behavior of the head loss due to flow-through decreasers.

A detailed analytical approach to the U.V.T. C calculation will be the subject of a paper in the near future.

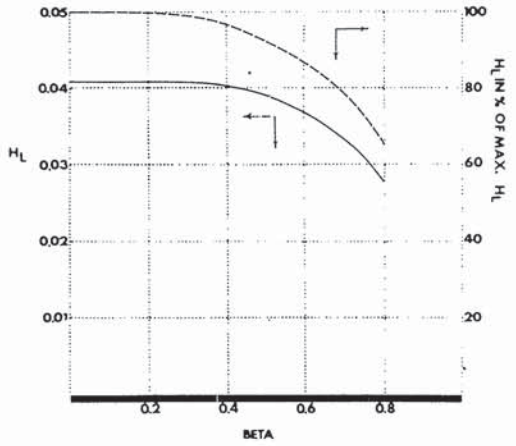

Fig. 12 H_L versus beta

2.2 Line Size Effect on C. Fig. 13 is a replot of the cast iron portion of the 51 mean C's. All these tubes had bronze throat liners and were not machined on the entrance and inlet cone section, thus representing the most homogeneous data group. The C deviation versus D plot shows no line size effect within a ± 0.5 percent twice standard deviation tolerance band ($13/A$), verifying the implication of equation (1) according to which C should be independent of line size.

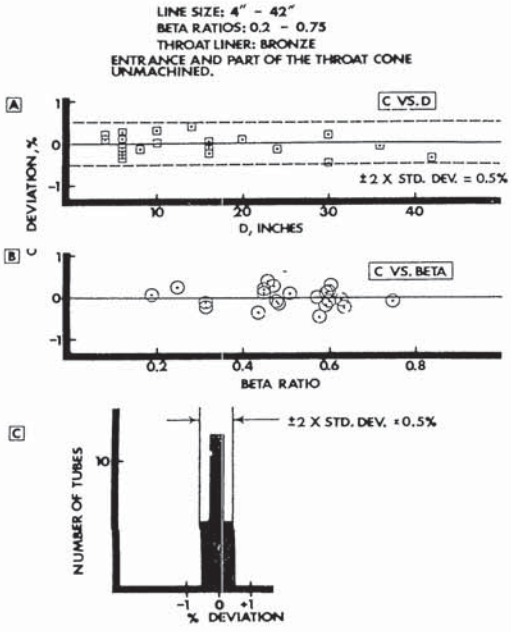

Fig. 13 Mean C data for 22 C.I. U.V.T.'s

2.3 Effect of R_D on C. The data referring to the R_D behavior of the U.V.T. C will be presented for the following practical and arbitrarily selected R_D ranges:

2.31 Low R_D—below 200,000. In Fig. 14, the deviations of single calibration points are shown from their respective constant value for "low" R_D's obtained on U.V.T.'s in the 1.5 to 18-in. line size and 0.31 to 0.75 beta range. All points were obtained with cold water calibration at Alden Research Lab and BIF's Lab. It must be mentioned that only such data have been used in the plot where the single calibration point tolerance [2] was half (or less) of the C deviation that was expected at a given R_D. The consequence of this policy is that the points plotted for lower R_D's belong, as a rule, to tubes of smaller line and/or beta size.

The data indicate C constancy down to about 75,000 R_D which is better than the 200,000 R_D limit given by reference [1] for Classical Venturi tubes.

This difference in performance should be caused by the difference in the shapes of the Classical Venturi and U.V.T. transition sections, making H_L in equation (1) behave differently as R_D changes; namely, for Classical Venturis H_L is composed mostly of friction loss generated by the long smoothly curved

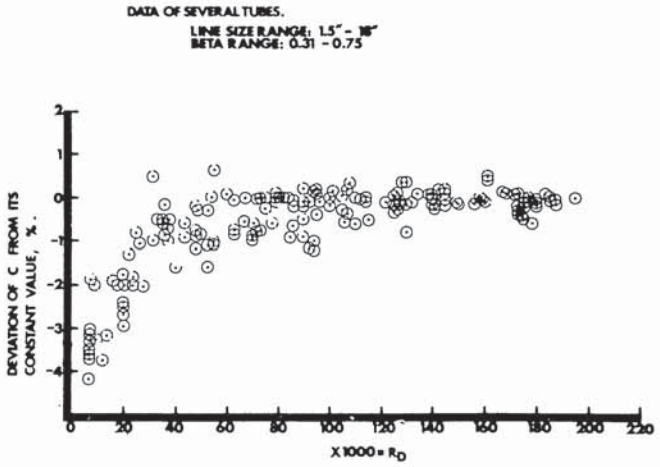

Fig. 14 Effect of R_D on coefficient; low R_D

transition section contour, whereas the U.V.T. H_L is caused, to a greater degree, by turbulence losses at the expansion of the vena contractae and to a lesser degree by friction loss in the much shorter transition section. Since friction loss increases and orifice type loss decreases as R_D diminishes, their effect tends to cancel each other, preventing the lowering of the C down to smaller R_D's.

2.32 Medium R_D 0.2 to 2.0 x 10^6. In Fig. 15, several calibrations of a 6-in. bronze U.V.T. are shown performed at Alden Research Lab. First, the tube was calibrated in the old facility with cold water in April, 1970. This calibration was repeated two and a half years later. At this time, the tube was calibrated in Alden Research Lab's new facility also with warm water.

These data, as well as all other U.V.T. calibrations, show no evidence of a hump attributed to boundary-layer transition for certain devices [6, 8, and 9]. The absence of the hump should be caused by the U.V.T. transition shape which locates the boundary-layer transition at its sharp wall contour change and keeps the boundary-layer turbulent down to lower R_D's by creating artificial turbulence, favorably influencing α_d in equation (1).

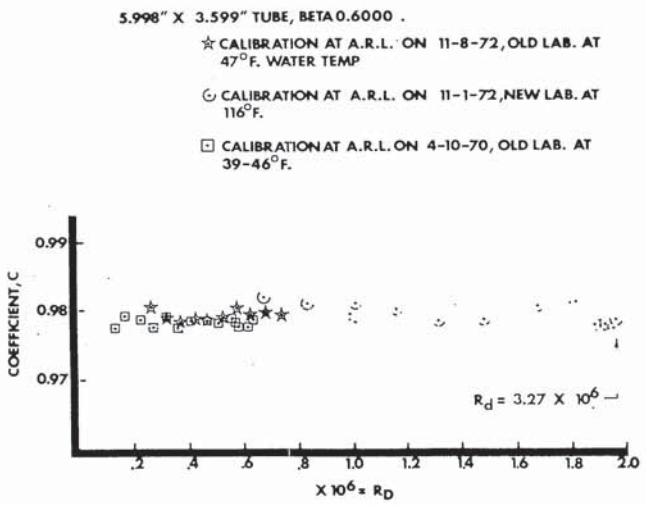

Fig. 15 Effect of R_D on coefficient; medium R_D

2.33 High R_D - over 2 x 10^6. Fig. 16 shows the calibration results for the highest R_D so far available for U.V.T.'s. This tube was calibrated on two independent tap sets located 180 deg apart. The data indicate no "C shape" from the lowest R_D to the highest one of 5.1 $\times$ 10^6 which corresponds to 7.7 $\times$ 10^6 throat Reynolds number.

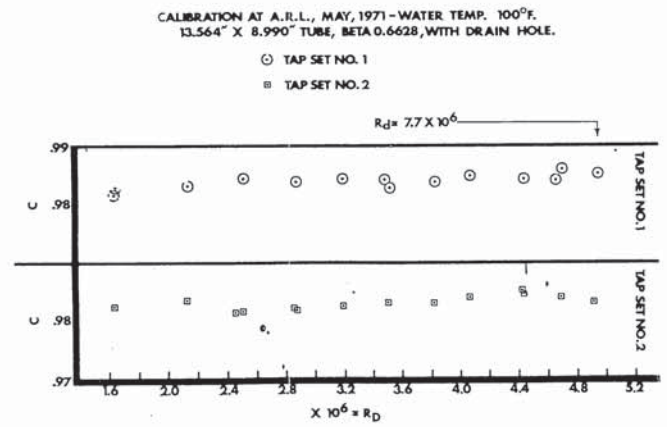

Fig. 16 Effect of R_D on coefficient; high R_D

This result can be expected from equation (1) based on what was said about α_d in Paragraph 2.32 and H_L in Paragraph 2.31.

Due to the scarcity of calibration data at extremely high R_D's, Fig. 17 deserves some interest.

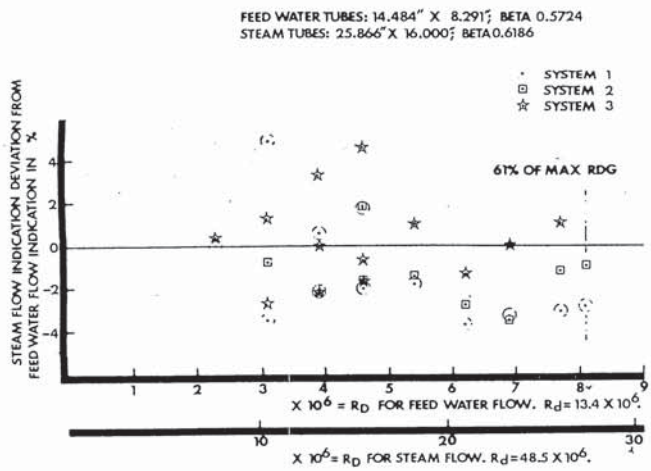

Fig. 17 Effect of R_D on C; high R_D

Here chart readings are presented which were obtained on three metering systems in a power plant. Each system consists of a calibrated feedwater U.V.T. and an uncalibrated steam U.V.T. with the same mass flow passing through them. The plots compare the steam flow readout to the feedwater readout. When reviewing the results, the large readout system tolerances should be kept in mind; namely, the tolerance of the feedwater tube C, feedwater transmitter and recorder and the steam tube C with its transmitter and recorder. Furthermore, the fact ought to be realized that instrumentation accuracies are given in percent of span; consequently, at lower rates, higher deviations should be expected.

2.4 Basic Accuracy of C, Calibrated (2). Since here no flow pattern effect is assumed on C, the only way device design can contribute to better accuracy is by not magnifying loop noise in its differential. Lesser differential fluctuation will hold down the single calibration point scatter lowering the standard deviation referred to the mean C; consequently, yielding smaller calibrated tolerances calculated by [2]:

$$\pm \text{ Tolerance} = \frac{t \times \text{Std. Dev.}}{\sqrt{N-1}} \qquad (2)$$

Hundreds of calibrations during the past five years evidenced low differential noise level for this device that could be expected since inlet and throat taps "see" true static pressure.

The standard deviations of mean C's, based on 10–14 single calibration points, were found to be between 0.07 to 0.20 percent.

Since equation (1) assured and the extensive calibrations substantiated no R_D effect on C at higher R_D's, the mean C of a calibrated U.V.T. becomes the average of the single calibration points obtained in the range of R_D where C constancy becomes obvious.

Based on the above facts and assuming no biased error in the calibrating equaipment and procedure, calibrated mean C accuracies for U.V.T.'s with 95 percent confidence level can be expected as follows:

N	=	10		14	
t	=	3.25		3.01	
Std. Dev. $\pm$ percent	=	0.07	0.20	0.07	0.20
Accuracy $\pm$ percent	=	0.08	0.22	0.06	0.17

2.5 Basic Accuracy of C, Uncalibrated. Twice standard deviation uncalibrated accuracies [1, 2] were calculated for different quality groups of U.V.T.'s, having single inlet and throat taps (no annular chambers).

Fig. 11 shows $\pm$0.75 percent accuracy for standard U.V.T.'s made of different materials by different manufacturing methods with partial machining of the entrance and transition section. The line size range is 3 to 42-in., beta range 0.2–0.75.

Fig. 13 refers to a more homogeneous group of the same data; namely, the cast iron tubes with bronze throat liner. It is interesting to note that the twice standard deviation of this group is $\pm$0.5 percent in spite of the fact that the entrance and inlet cone sections of the tubes were unmachined. Also, it is worthwhile to emphasize that the calibrations cover 4 to 42-in. line size and 0.2–0.75 beta range.

Since no device is known by author which achieved $\pm$0.5 percent true twice standard deviation accuracy for the wide line size and beta range shown in Fig. 13, the need arose to further substantiate the actual findings. This attempt is made in Fig. 19 for a 0.5 beta C.I. U.V.T. In this figure, the C effect of manufacturing tolerances are estimated for different portions of the tube hydraulic shape. The root sum square (RSS) value of the manufacturing tolerance effect was found to be $\pm$0.35 percent.

The accuracy of a typical water calibration is estimated also based on the RSS value of the main tolerance sources which are:

- the always present effect of piping,
- single calibration point scatter, *and*
- errors due to manometer setting, reading, etc., at lower differentials, unavoidable at larger tube calibrations.

It is important to note that the calibration accuracy is ± 0.25 percent, thus a very significant portion of the total tolerance.

This analysis warrants ± 0.43 percent accuracy which agrees well with the ± 0.5 percent actual one, especially when it is realized that Fig.. 13 includes many tubes with larger than 0.5 percent beta for which the analytically determined tolerance is somewhat greater.

Further insight can be gained into the formation of the twice standard deviation accuracy from Fig. 18 where the calibration results are summarized for 19 special quality U.V.T.'s. These tubes were specials because their transition and throat sections were made of stainless steel with full machining and had two $^3/_8$-in. radius drain holes where leak flow occurred. All these tubes were calibrated on two tap sets simultaneously at Alden Research Lab in the R_D range of $1\text{–}5.0 \times 10^6$.

The twice standard deviation was found to be ± 0.42 percent. The differences between C's as obtained on opposite sides for each tube are plotted also showing that most of them were below 0.25 percent.

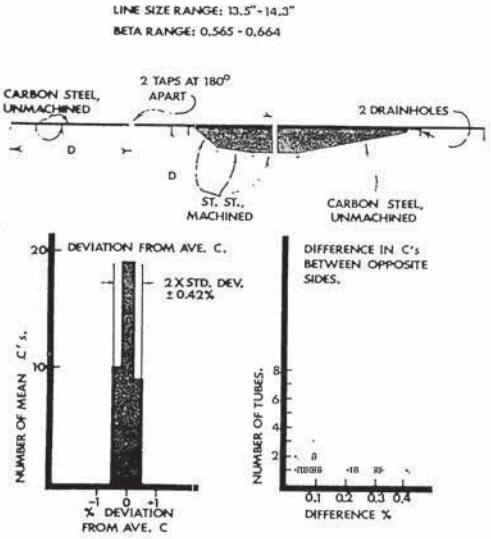

Fig. 18 Calibrated mean C data for 19 special quality U.V.T.'s (based on 550 calibration points)

For proper appreciation of the results, it should be mentioned that the entrance sections of these tubes were unmachined carbon steel, some of the beta ratios were as high as 0.664, the transition and throat sections were machined to about 64 microin. surface finish only, and all these tubes had leak flow through their drain holes whose geometry could not be controlled accurately.

For the excellent twice standard deviation results experienced with U.V.T.'s, the following explanation is given:

(*A*) The inlet tap location is a function of beta; thus it keeps its hydraulic meaning.

(*B*) The transition section is short and sharply shaped with no smooth blending radii; consequently:

- the head loss caused by it becomes practically independent of surface finish;
- the throat flow mechanism is controlled consistently by the transition section — axially the flow pattern-wise which is not the case when blending radii of different magnitudes are used.

(*C*) The throat entrance and exit design due to the sharp wall contour change holds the vena contracta in the same place and at nearly the same magnitudes.

(*D*) The throat length and design provides symmetrical axial throat wall pressure distribution about the throat tap having always the same shape (no uncertain blending radii), thus diminishing the effect of manufacturing tolerance on the tap location.

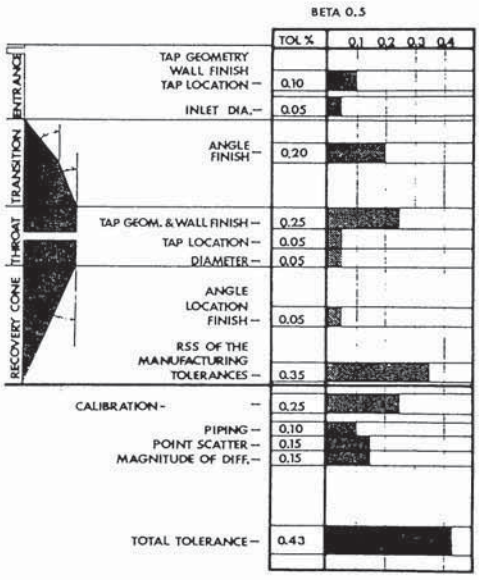

Fig. 19 Tolerance calculation for C.I. U.V.T.'s with bronze throat liner.

2.6 Derived Designs. Fig. 3(*b*) shows the following derivations of the basic U.V.T. hydraulic shape.

2.61—Nozzle Design With Throat Taps. The limited test data available to date on this design indicates about 0.2 percent C increment due to the elimination of the recovery cone and naturally greater head loss. The behavior of C and the value and behavior of Y are the same as those of normal U.V.T.'s.

2.62—Nozzle Design With Pipe Taps. Three such devices were built and calibrated with small beta ratios in 16, 30, and 42-in. line sizes. C values were the same as that of standard U.V.T.'s, indicating similar characteristics as described before for standard tubes except head loss which, of course, is greater.

2.63—Rectangular Design. The detailed discussion of the rectangular U.V.T. shall be the subject of a future paper. It is interesting to report, however, that so far two prototypes were built based on the principle of "equal axial acceleration." A circular and rectangular tube has "equal axial acceleration" when their area ratios are the same at each sharp change of the tube contour, and the axial distance between corresponding tube contour changes are the same when expressed in inlet pipe diameter or for rectangular tubes in terms of equivalent pipe diameter where:

$$\text{Equivalent pipe dia} = \sqrt{\frac{\text{Area}}{\frac{\pi}{4}}} \qquad (3)$$

The calibrations resulted C values within 1 percent of the circular one, R_D behavior similar to that of circular tubes, and head loss values about 20 percent above the circular one with recovery cones having two sides parallel and 14-deg included angle for the other sides.

Part 2—Installation Effect, Compressible Flow, and Head Loss

2.7 Installed Accuracy. In this paragraph, some of the test results are presented which show the effect of upstream and downstream piping on the metering performance of UVT's with single inlet and throat taps.

A unique feature of most of these tests is that two manometers were used simultaneously at each run: one was measuring the differential between the static inlet and throat tap, the other between the corner inlet tap and throat tap. This method yielded the advantage of not only providing piping effect data for corner tapped UVT's, but gave a better understanding of the error generation in the device which knowledge can be extrapolated to other types of differential producers.

To assure unbiased C deviation statements, they were made in the following manner:

For each tube and for each piping configuration, the C deviation values are the means of three single runs taken at flow conditions where the single point accuracy was the best.

2.71 Most Common Upstream Effects. Fig. 20 shows the effect on C of a 4 $\times$ 6 in. increaser in the function of beta ratio, distance between the increaser and the tube and type of inlet tapping (static or corner).

Fig. 21 is similar data for an 8 $\times$ 6 in. decreaser preceding the tube.

Fig. 22 shows the effect of a 6-in. short radius elbow in a similar way, except here attention is paid to the orientation of the taps in relation to the plane of the elbow.

Based on Figs. 20, 21, and 22, the following important conclusions can be drawn:

(A) C deviation increases with increasing beta ratio.

(B) Corner inlet taps yield significantly greater C deviations than static inlet taps.

(C) Piping effect diminishes with increasing Z distance.

Extensive tests have been run on the effect of two direct coupled 6-in. short radius elbows in orthogonal planes on the performance of 6-in. UVT's with 0.45, 0.60, and 0.72 beta ratios. These tubes had single throat taps with varied inlet taps, i.e., static tap, single and externally manifolded, corner tap

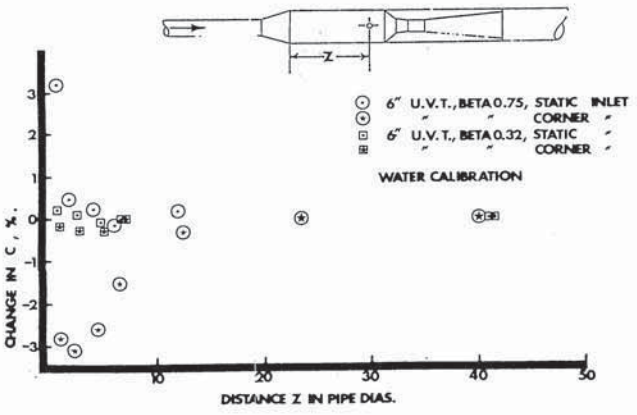

Fig. 20 Effect of a 4 X 6-in. increaser

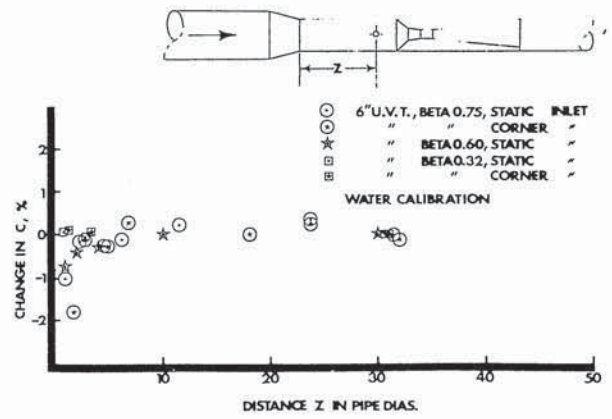

Fig. 21 Effect of a 8 X 6-in. decreaser

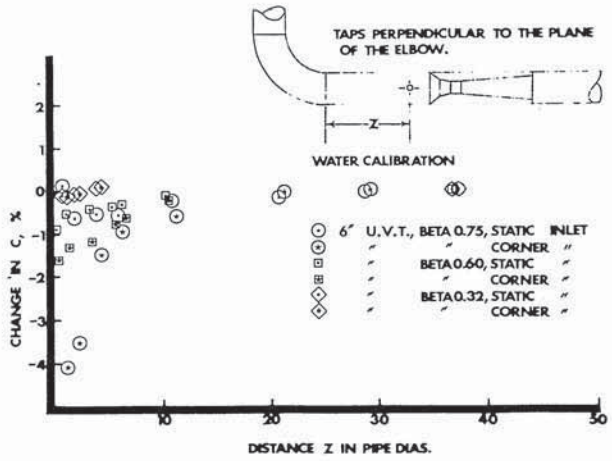

Fig. 22 Effect of a 6-in. short radius elbow

with large volume internal annulus. To save space, only the 0.6 beta test results are shown in Fig. 23; while from the rest of the tests, only the conclusions are given. In each position, the effect of orientation was explored with some checks of different type straighteners (tubular, sector) and no straightener at all. Based on Fig. 23 and the rest of the tests, the following summary can be given:

(A) Inlet corner taps yield larger C change than static taps.

(B) Manifolding the inlet taps cuts down orientation sensitivity, but does not eliminate C error.

(C) The effect of orientation is evident and diminishes with decreasing beta ratio.

(D) The effect of orientation is uniform ($+C$ change stays $+$, $-$ stays $-$) with sector or tubular type straightener at different Z distances, whereas the direction of C change varies without the straightener.

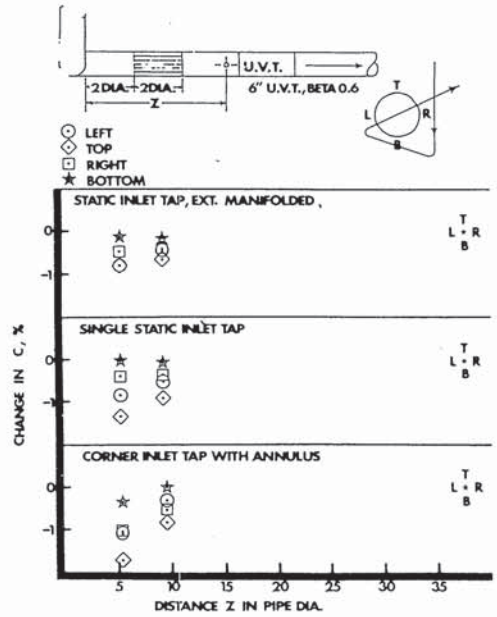

Fig. 23 Effect of two 6-in. short radius elbow direct coupled in orthogonal planes

(*E*) The tubular straightener (18 tubes) at the 6-dia Z distance caused somewhat larger orientation sensitivity than the sector type vane (six triangular sectors) for the 0.72 beta tube. The change in C was somewhat greater also.

(*F*) The 0.45 veta tube with single tap revealed neither C change nor orientation sensitivity in the 6-dia Z position with or without straightener.

(*G*) C change diminishes with increasing Z distance.

The findings yield the conclusion that the best way to achieve accurate metering under these conditions is to use small beta with no vane.

2.72 Orientation Effect. Fig. 24 shows the effect of orientation on the C of a 0.75 beta UVT after a 6-in. short radius elbow.

The data explains why even well-designed annular chambers cannot yield the normal C, "averaging out" the side effects because the average of the C deviations on the sides is not equal to the normal C.

Another important teaching of this figure is that even well-designed annular chambers will provide different C deviations in case of nonaxisymmetrical flow patterns when located at the same Z distance, but have different tap arrangements in regard to their number and orientation.

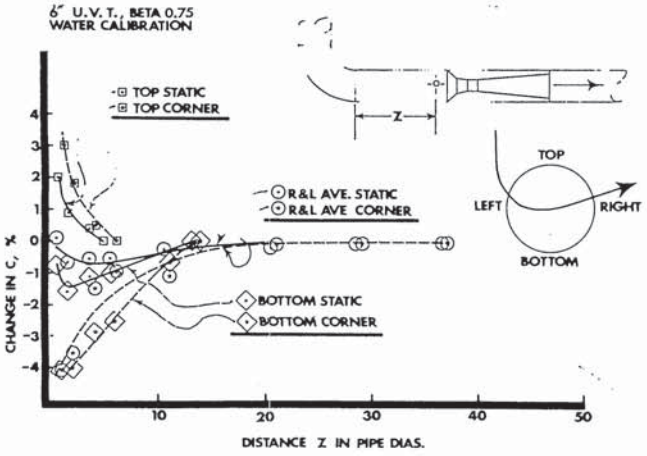

Fig. 24 Orientation effect of a 6-in. short radius elbow

2.73 Straightener Effect. Fig. 25 shows the detrimental effect of an improperly used straightener.

After the short radius elbow, the asymmetrical velocity profile is preserved and stablized by the tubular type straightener (sector straightener acts similarly), causing greater orientation sensitivity than the one observed with tube in the same position relative to the elbow, but without the straightener.

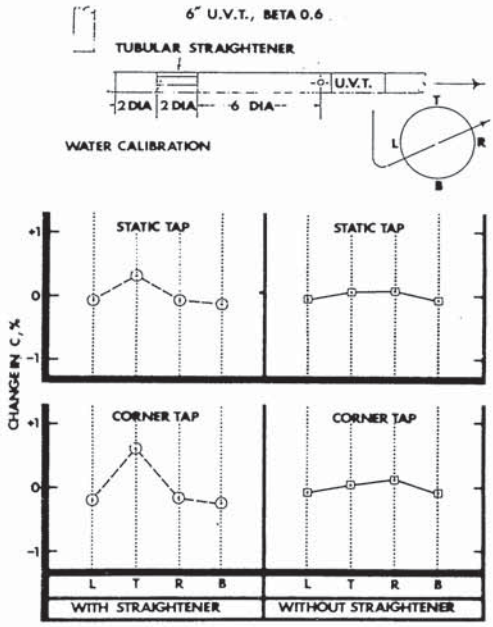

Fig. 25 Effect of a straightener

While these data are interesting, it gains importance in view of the fact that metering "codes" approve installations as shown in Fig. 25.

2.74 Downstream Effect. Fig. 26 shows the results of tests checking into the effect of downstream piping on the C of UVT's.

A gate valve was directly coupled to the downstream flange of the 0.75 and 0.32 beta 6-in. UVT's. C deviations were established then by setting the gate valve to different openings. The data scatter shown in the figure is not greater than the test tolerance; consequently, it can be stated with confidence that these tubes with recovery cones are insensitive to downstream piping.

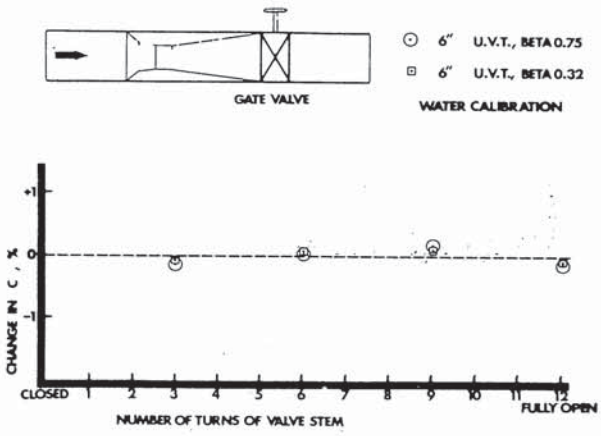

Fig. 26 Effect of downstream piping

2.75 The Validity of Hydraulic Similitude. Fig. 27 gives information on the frequently asked question about the reliability of the principle of hydraulic similitude.

To test the theory, a 6 and a 12-in. metering system were built in strict geometrical similitude as shown. Both systems consisted of a miter bend, close coupled to a wide open symmetrical disk Butterfly valve followed by a 0.75 beta UVT with corner inlet taps in one case at 0.13 pipe diameter distance, in the other at 0.5 diameter distance. The 6-in. system was calibrated at BIF's Hydraulic Lab, the 12-in. system at Alden Research Lab.

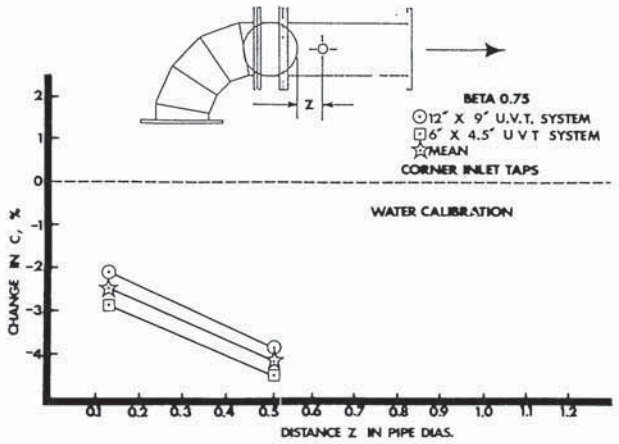

Fig. 27 The validity of hydraulic similitude

As can be seen (Fig. 27), both systems showed the same C change in the function of distance Z, while the C values as found at the different locations by the different labs are within ± 0.38 percent at the 0.13-dia location and within ± 0.32 percent at the 0.5-dia location from the mean value. These deviations, especially in view of the large beta ratio (0.75) of these tubes and of the fact that the standard uncalibrated accuracy of normally installed UVT's with corner inlet tap is ± 1 percent, must be considered as proof to the usefulness and validity of properly conducted model tests.

2.76 The Stability of C. Another important question in connection with "bad" approach piping is the stability of C in the function of R_D; namely, will C stay constant at higher R_D's once it has become so at lower ones?

In order to investigate this point, the 12-in. elbow, Butterfly valve, 0.75 beta UVT system was calibrated first at Alden Research Lab's old facility with cold water; then the whole setup was transferred to the new lab and calibrated with warm water.

The test result is shown in Fig. 28 and indicates no shape (see Fig. 2) in the C versus R_D relation once C became constant at low R_D's.

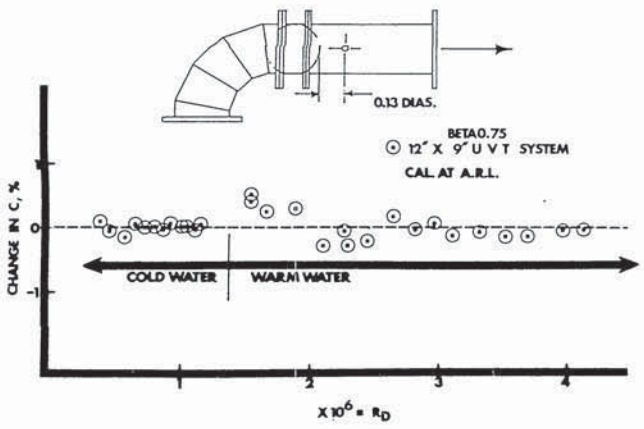

Fig. 28 "C" Stability

2.77 Effect of Line Fluid. Another much questioned aspect of installation effect investigations is the effect of change in line fluid on C errors caused by the same abnormal flow pattern. To throw some light on this question, a test was conducted (Fig. 29) on a 0.75 beta 6-in. UVT whose C was determined by using water with normal upstream piping, then with a 0.746 beta orifice plate installed two pipe diameter distance upstream of the tube. The change in C was found to be +7.7 percent.

The same test was repeated by air as line fluid. Here the "actual" airflow was determined by a water-calibrated orifice plate test section using the ASME [1] expansion factor. Atmospheric air was moved by a blower. The effect on C of the same upstream piping change was +4.6 percent significantly and meaningfully less than the one found by water as line fluid.

The cause of the smaller C deviation with air, in the author's opinion, should be looked for in the greater self-normalizing ability of compressible flow.

If the above finding was typical for other "bad" upstream pipings and the reasoning is correct, then the conclusion becomes evident that upstream piping effects obtained by water exaggerate the C changes that can be expected for compressible fluids.

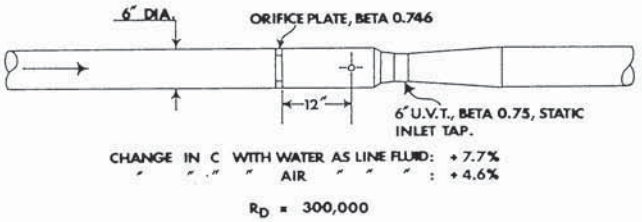

Fig 29 Line fluid versus upstream piping effect

2.8 Effect of Cavitation Number (σ) on C. To obtain a better understanding of the effect of cavitation on the flow mechanism in the tube as well as on its C a 6-in. size, 0.4 beta transparent UVT was built on plexiglass and tested at BIF's Hydraulic Lab with cold and warm water. At each test run, the throat static pressure, P_d, was accurately measured by a mercury manometer, while the rate of flow was established by collecting the water in a volume tank; thus the actual average throat velocity, V_d, could be calculated:

$$V_d = \frac{\text{Actual CFS}}{\text{Throat area}} \tag{4}$$

Fig. 30 shows the observations made and C's obtained at each test run plotted in the function of a so-called cavitation number:

$$\sigma = \frac{P_d - P_w}{\frac{V_d^2}{2g}} \tag{5}$$

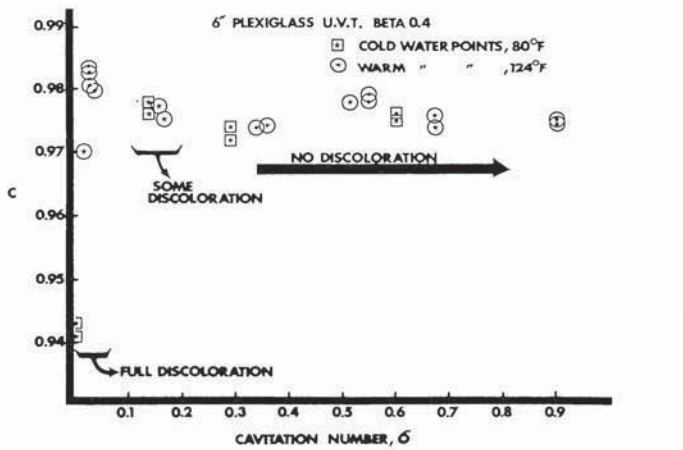

Fig. 30 Cavitation Investigation

While the effect of σ on C can be easily read from Fig. 30, the following explanation is given to facilitate the understanding of what had been observed visually:

Some discoloration, which began to appear below 0.2 σ value, means definitely descernible white rings visible right at the sharp intersection lines of the tube contour—having less than $^1/_{32}$-in. width. As σ was lowered, the rings widened, extending downstream of the initial cross section which stayed in place.

No discoloration means, no visible sign to the fact that water flow takes place in the tube.

Below $\sigma \approx 0.05$, the portion of the tube from the intersection of the inlet and throat cone (Fig. 3(*a*)) to well in the recovery cone became fully discolored. But in spite of the drastic change in appearance, C deviation could not be observed down to 0.025 σ value, below which C changed significantly.

It is interesting to note that at $\sigma \approx 0.006$, the head loss measured across the tube (at two pipe dia upstream and eight pipe dia downstream taps) doubled.

2.9 Hydraulic Shape Sensitivity of C. To check the hydraulic shape sensitivity of the UVT C, the following tests have been performed:

2.91 Effect of the Inlet Cone Angle Change. The inlet half cone angle of a 6-in. 0.75 beta UVT was changed from 50 to 30 deg increasing the C by 1 percent for the static inlet tap and 1.4 percent for the corner inlet tap.

The inlet cone half angle was changed from 50 to 40 deg for a 6-in. 0.32 beta UVT causing a 0.3 percent increment in C for both static and corner inlet taps.

2.92 Effect of Surface Finish Change. The inlet cone surface finish as well as I.D. was changed from 20 to 1000 μ in a 0.75 and 0.32 beta 6-in. UVT by painting the surfaces with a mixture of sand and epoxy glue (about $^1/_{32}$-in. thick layer). Both C's lowered by the same amount for static and corner taps (as was expected). The C change was -0.40 percent for the 0.75 beta tube, -0.12 percent for the 0.32 beta one.

Next the inlet half length of the throat cones were painted in the same manner changing surface finish as well as I.D. The C of the 0.75 beta tube changed by -0.7 percent, that of the 0.32 beta tube by -0.75 percent.

2.93 Effect of Tap Hole Geometry. In a 6-in. UVT with 0.6 beta, four inlet and four throat taps were located 90 deg apart. The holes had different diameters and diameter to hole length ratios.

The test results indicated no inlet tap geometry effect, while the throat tap tests verified the necessity of the 1.5 to 2 hole length to diameter ratio for undistorted static pressure sensation, as mentioned in reference [1].

3 Compressible Flow Tests

3.1 Subsonic Flow. Since the UVT senses true inlet and throat static pressures similarly to Classical Venturi tubes, its adiabatic expansion factor can be calculated by the formula given for Y in reference [1] for Venturi tubes and Venturi nozzles.

The magnitude and behavior of the tolerance on Y is also similar to that of Classical Venturis (1).

To prove the validity of the above statements, airflow tests were conducted at BIF as well as at C.E.E.S.I. Labs.

At BIF the "actual" airflow rate was established by a water-calibrated orifice plate test section with a C tolerance of ± 0.5 percent and Y tolerance of 0–0.75 percent (proportional to x) per reference [1].

At C.E.E.S.I., the "actual" flow rate was determined by pre-calibrated choking nozzles. The estimated testing accuracy was ± 0.5 percent.

In Fig. 31, the results of these tests are shown, in terms of deviation from water C (ΔC), percent, versus x.

Where,

$$\Delta C = \left(\frac{C \text{ established by air calibration}}{C \text{ established by water calibration}} - 1 \right) 100 \tag{6}$$

On the plot, the tolerance bands are also shown. As can be seen, most of the points are well within the applicable tolerance bands for the full x value range of 0–0.4.

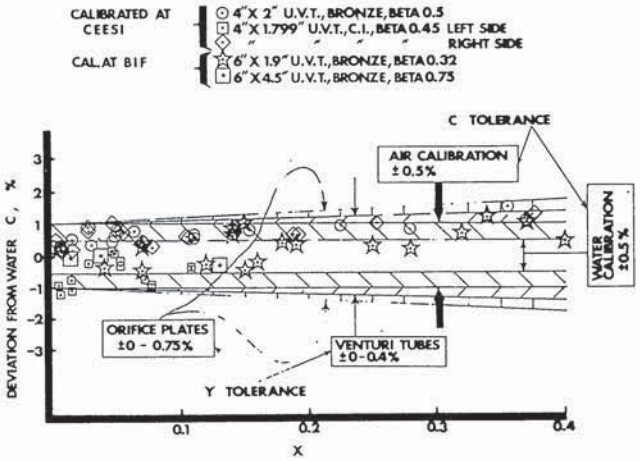

Fig. 31 Verification of the adiabatic expansion factor (Y)

3.2 Choking Flow Tests. Fig. 32 is the summary of choke flow test results conducted at C.E.E.S.I. on five 4-in. devices. The important device dimensions and beta ratios are shown on the figure with the calibration points.

While a more penetrating analysis of the results shall be presented in a future paper, the following interesting observations can be made already:

(*A*) The drastic change in geometry between (radial) design 1 and design 2 caused only a 0.25 percent difference in the C.

(*B*) Changing the 30-deg inlet cone half angle (design 2) to 40 deg (design 3) caused 0.8 percent C change.

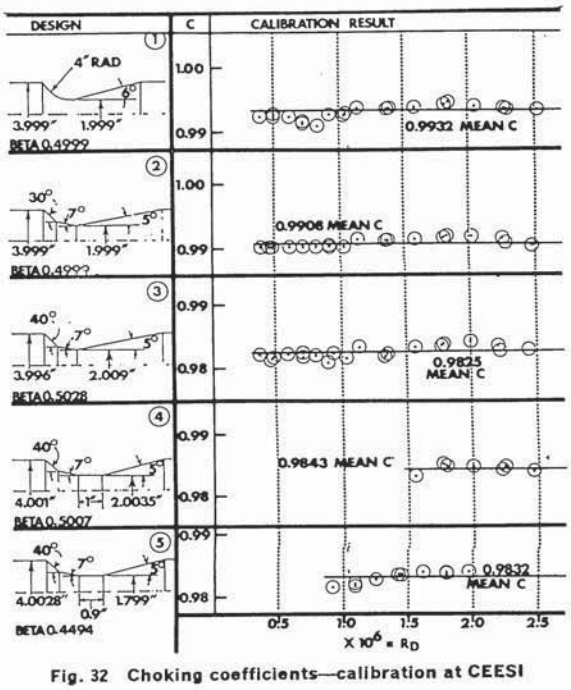

Fig. 32 Choking coefficients—calibration at CEESI

(*C*) Comparing the choking *C*'s for design 3, 4, and 5 indicates practically no effect of the addition of a cylindrical throat on the choking *C*.

(*D*) The R_D sensitivity of the choking *C* of the radial device (design 1) is definitely not better than that of the UVT type shapes in the R_D range tested.

4 Head Loss Investigation

An extensive investigation of the permanent head loss properties of the UVT hydraulic shape had been performed revealing the following results.

4.1 Effect of Recovery Cone Truncation. To thoroughly investigate the effect of recovery cone truncation on the permanent head loss two pieces of new 8-in. carbon steel pipe were used upstream and downstream of a 0.4, 0.6, and 0.725 beta plastic insert center flanged UVT's. These tubes had almost fully extended recovery cones truncated only slightly to permit insertion into the pipe (Fig. 33). Head loss caused by the hydraulic shape of the tube was established by subtracting the pipe loss measured between the head loss taps with the tube removed, from the loss observed between the same taps with the tube in place. These hydraulic shape losses were established at two extreme R_D's that could be provided with sufficient accuracy at BIF Hydraulic Lab. In Fig. 33, values obtained at the highest R_D's are plotted. To establish the effect of truncation, portions of the recovery cones were just sawed off for repeated head loss tests.

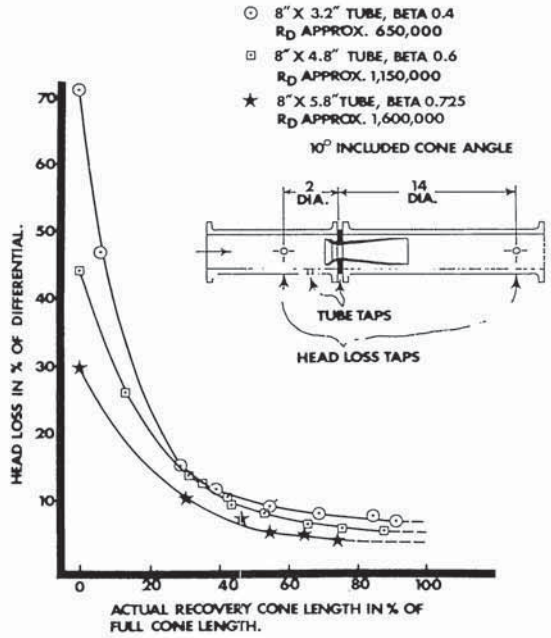

Fig. 33 Head loss versus recovery cone truncation

After each truncation, *C* was also checked indicating no *C* change, except in the case with no recovery cone with a +0.2 percent *C* change was observed.

The results are summarized in Fig. 33 yielding the following conclusions:

(*A*) A large portion of the recovery cone can be removed without significantly increasing the permanent head loss.

(*B*) No amount of truncation decreased the head loss [3, 10]. In other words, as soon as the cone was truncated the head loss grew.

(*C*) Shortening the recovery cone by truncation has no effect on *C*.

4.2 Effect of R_D. The effect of R_D on the permanent head loss caused by different tube hydraulic shapes is a very poorly investigated subject, especially if the effect of a wide change in R_D is considered [3, 10]. The head loss percent, whether it is percent of differential or of inlet velocity head, may increase, decrease, or stay the same depending on device geometry as R_D increases. To know its behavior, consequently, may become important where energy economy is required at high R_D applications.

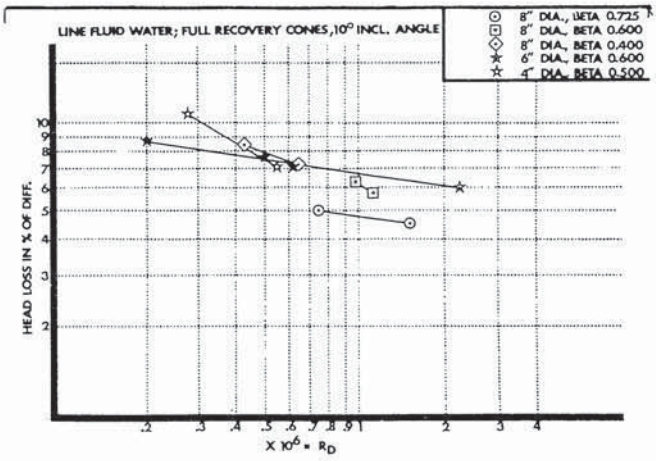

Fig. 34 Head loss versus R_D for U.V.T.'s

Fig. 34 presents test data obtained with water as line fluid for several UVT's having full recovery cones with different lines sizes and beta ratios. All data indicate sharply descending values for UVT's as R_D increases, making head loss estimates for high R_D's conservative when percent values established at low R_D's are used. The head loss of tubes having truncated recovery cones behave similarly.

4.3 Effect of Surface Roughness. The effect of recovery cone surface roughness on the permanent head loss was studied on a 4.001 × 2.0035 bronze UVT (beta = 0.5007) having fully extended recovery cone with 10-deg included angle. Head loss was established for this tube in BIF's lab in as-machined condition with a 25 microin. (rms) surface finish on the recovery cone. Then the full recovery cone was painted with epoxy glue-sand mixture. The surface roughness was measured to be 1700 microin. Head loss was checked again. The test results are shown in Fig. 35 and indicate:

(*A*) About 29 percent increment in head loss due to the roughening of the surface at the higher R_D.

(*B*) Smaller R_D effect on the head loss in the lower R_D range for the rough cone. This behavior is due to the fact that the skin friction loss becomes more and more R_D independent as the pipe wall surface becomes rougher.

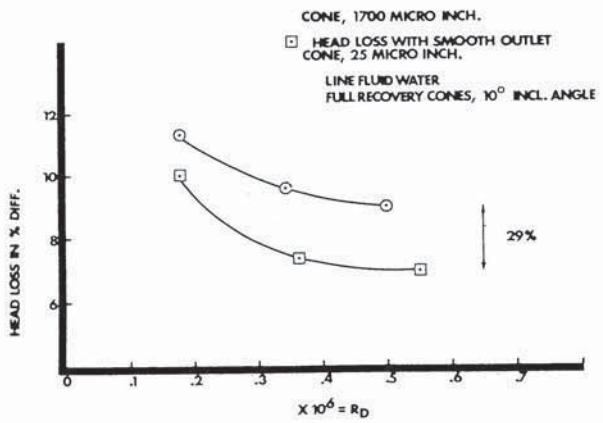

Fig. 35 Head loss versus recovery cone surface roughness

LINE FLUID WATER

4.4 Effect of Beta Ratio. In Fig. 36, the head loss data of the plastic tubes for full recovery cones is summarized from Fig. 33. The head loss in percent of differential grows as beta decreases as is the case for any differential producer.

Test data from reference [10] for Classical Venturi tubes with several recovery cone angles are also shown in Fig. 36, indicating significantly lower losses for UVT's than was found for Classical Venturis for any cone angle.

The investigation was further pursued by testing a 4-in. cast iron 0.45 beta Classical Venturi tube having fully extended recovery cone with 14-deg included cone angle at the same time and in the same pipe with a 4 in. cast iron 0.45 beta UVT with 10-deg (included angle) recovery cone with 50 percent truncation. The hydraulic shape loss of the Classical Venturi tube was found to be 16.7 percent that of the UVT, 9.5 percent (Fig. 38).

These findings are considered to support the following conclusions: The head loss caused by the UVT hydraulic shape is smaller than that of the Classical Venturi tubes because:

(*A*) The length of cylindrical throat section for UVT's is half of that of Classical Venturis, causing lesser skin friction loss in the high velocity region.

(*B*) The flow entering the recovery cone is "conditioned" by the UVT transition and throat section improving the efficiency of the recovery cone (higher turbulence level, blunter velocity profile) which is apparently not the case with the Classical Venturi.

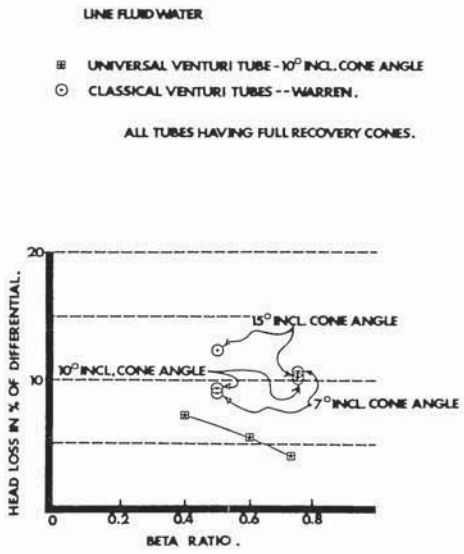

Fig. 36 Head loss versus beta ratio

4.5 Data Interpretation. The customary way of stating head loss caused by differential producers is in percent of differential. While this method has some merit, it becomes entirely useless when the true efficiency of different hydraulic shapes is to be measured or compared. Why? Because the magnitude of the differential produced by different hydraulic shapes may be drastically different at the same rate of flow, in the same pipe with tubes having the same beta ratio [2].

One proper way of describing the efficiency of different tube hydraulic shapes would be to express them in percent of inlet velocity head instead of percent of differential. This method has, however, one practical disadvantage; namely, it requires the calculation of the inlet velocity head in a commonly useful unit, like inches of water at 60 deg F, and 14.7 psia or in psi. To do this may become troublesome, but since the differential must be calculated anyway, it becomes available in practical units.

Fig. 37 resolves this problem in the following manner: The head losses in percent of differential are shown in dashed lines for Classical Venturi tubes [10], Low Loss tubes [3], and UVT's. The solid lines then are showing head losses in percent of such a differential which would be produced by a given tube if its C was unity, thus:

$$\text{Head loss, corrected for } C = 1 = \frac{\text{Head loss percent of actual diff.}}{C^2} \quad (7)$$

Presenting and/or comparing the head loss for different tubes in this manner is convenient becasue C is known and clears up the question, permitting proper technical evaluation of the efficiencies of different hydraulic shapes which accelerate and decelerate flow.

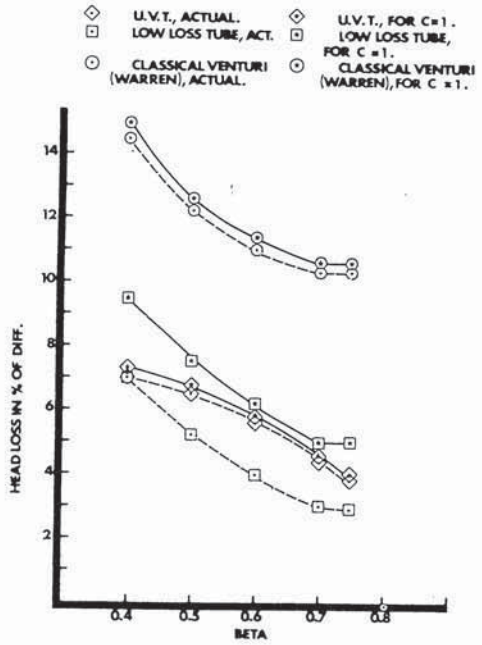

Fig. 37 Head loss; interpretation and comparison

4.6 Loop Noise Versus Hydraulic Shape. An interesting observation is presented in Fig. 38 about the loop noise generating properties of a 4-in. cast iron UVT beta = 0.45 with 10-deg (included angle) recovery cone, having 50 percent truncation and that of a 4-in. cast iron Classical Venturi tube of the same beta ratio having 14-deg (included angle) fully extended recovery cone.

Fig. 38 shows the peak-to-peak head loss fluctuation as observed on a mercury manometer with $^7/_{16}$-in. bore connected to pipe taps located at two pipe diameters upstream and ten pipe diameter distance downstream of the tubes.

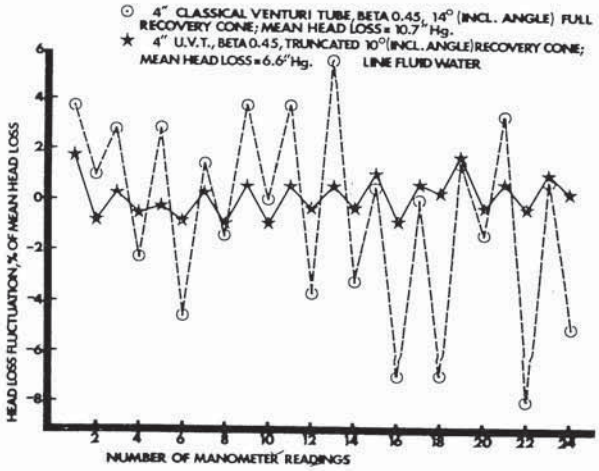

Fig. 38 Loop noise versus hydraulic shape

In the absence of a proper instrument, manometer readings were taken in pairs recording the highest and lowest mercury levels that appeared in the manometer at a time. Then the peak-to-peak fluctuations were calculated and plotted in terms of percent of the average head loss reading.

Interesting to note is the much smaller UVT head loss fluctuation in spite of the fact that the discharge diameter of the UVT recovery cone was only 2.9 in. as opposed to the Classical Venturi's full 4 in.

5 Conclusions

5.1 According to the test results presented in this paper, the goal set out in the introduction was achieved; namely, a new tube was developed which combines Classical Venturi tube type metering performance with short laying length and low head loss.

5.2 The development work followed thus satisfies the philosophy and method laid down in reference [2], providing the necessary information for the reliable application of the device for incompressible and compressible flow metering for wide line size, beta, and R_D range.

5.3 Some of the observations during the development work and achievements during the experience of the past five years deserve emphasis due to their novelty and/or importance.

5.31 Hydraulic Shape. The UVT hydraulic shape does not have smooth blending radii, which is a drastic deviation from the Classical tube design principle and practice. Some important performance characteristics discussed in the following paragraphs can be directly attributed to this hydraulic shape; interestingly, none could be found detrimental to metering performance so far.

5.32—R_D Sensitivity. In view of teachings found in some advanced papers on the occurrence of boundary-layer transition (with respect to R_D and axial location) and its effect of shaping the C versus R_D curve, the R_D sensitivity of the UVT must be considered extremely good. This feature, following the same theories, can be attributed to the tube hydraulic shape which trips the boundary layer at the same location and makes it turbulent at lower R_D's for the throat tap.

5.33—2 x Standard Deviation Tolerance. According to the evidence of the five years' experience with UVT's to achieve safely ± 0.5 percent uncalibrated basic accuracy is comparatively easy, not requiring close manufacturing tolerances on the entrance and transition sections. This feature again is due to the hydraulic shape as was pointed out in Paragraph 2.5.

5.34—Effect of Cavitation. In spite of the abrupt wall contour of the UVT, its C is not more sensitive to low cavitation numbers than well-rounded Classical Venturi tubes [12].

5.35—Inlet Static Versus Corner Taps. The tests proved beyond doubt that corner inlet taps are influenced by bad flow patterns to a greater extent than inlet static taps—a finding which refers to any kind of tube.

5.36—Use of Straighteners. The tests also indicated much greater C orientation sensitivity, in case of asymmetrical flow pattern, with tubular or sector type straighteners than what was observed without them. This is another finding that deserves general attention.

5.37—Head Loss. When the test data obtained by author for UVT's is compared to the head loss information available for other devices from ASME publications, a meaningful difference can be observed on behalf of the UVT when head loss is expressed in percent of the "corrected differential" or in terms of inlet velocity head. These index numbers describe the efficiency of the different hydraulic shapes in accelerating and decelerating flow. While in the author's opinion the magntiudes of the differences have no practical significance on most of the installations, they are still interesting from a scientific point of view.

5.38—Choking C. The choking flow data presented in the paper indicates the usefulness of different UVT designs for critical flow metering at the same time providing the possibility to correlate choke flow C value and behavior with device hydraulic shapes.

Nomenclature

C = coefficient of discharge
R_D = pipe Reynolds number
d = throat diameter
D = inlet diameter .
R_d = throat Reynolds number
α_d = actual throat kinetic energy content $\div \frac{V^2 d}{2g}$
α_D = actual inlet kinetic energy content $\div \frac{V^2_D}{2g}$
H_L = head loss occurring between inlet and throat tap, ft of line fluid $\div \frac{V^2 d}{2g}$
N = number of single calibration points
t = student's t
P''_L = local wall pressure, in. of water, at 14.7 psia, 60 deg F
P''_D = inlet static pressure, in. of water, at 14.7 psia, 60 deg F
h_w = differential pressure, in. of water, at 14.7 psia, 70 deg F
σ = cavitation number = $\frac{P_d - P_w}{\frac{V_d^2}{2g}}$
$\beta = \frac{d}{D}$
P_d = throat static pressure, ft of line fluid
P_w = fluid vapor pressure at throat temperature, ft of line fluid
V_D = average inlet velocity, ft/sec
V_d = average throat velocity, ft/sec
g = local acceleration due to gravity
Y = adiabatic expansion factor for Venturi tubes from reference [1]
x = $\frac{\text{differential pressure}}{\text{inlet static pressure}}$
ΔC = C deviation in percent
Z = distance

References

1 ASME: *Fluid Meters*, 6th edition, 1971.

2 Halmi, D., "Practical Guide to the Evaluation of the Metering Performance of Differential Producers," ASME Paper No. 72-WA/FM-2.

3 Hooper, L. J., "Design and Calibration of the Low Loss Tube," ASME Paper No. 61-WA-80.

4 Miner, I. O., "The Dall Flow Tube," ASME Paper No. 54-A-139.

5 Hooper, L. J., "Calibrations of Six Beth-Flow Meters at Alden Hydraulic Lab.," Worcester Polytechnic Institute, ASME Paper No. 49-A-38.

6 Hall, G. W., "Application of Boundary Layer Theory to Explain Some Nozzle and Venturi Flow Peculiarities," *Proc. Instn. Mech. Engrs.*

7 Ferron, A. G., "Velocity Profile Effects on the Discharge Coefficient of Pressure Differential Meters," ASME Paper No. 62-Hyd-8.

8 Cotton, Schofield, and Carcich, "Experience With Throat Tap Nozzles for Accurate Flow Measurement," *Journal of Engineering for Power*, TRANS. ASME, Vol. 94, Series A, No. 2, April 1972, pp. 133–141.

9 Cotton, K. C., and Westcott, J. C., "Throat Tap Nozzles Used for Accurate Flow Measurements," ASME Paper No. 59-A-174.

10 Warren, J., "A Study of Head Loss in Venturi-Meter Diffuser Sections," ASME Paper No. 50-A-65.

11 Numachi, F., Kobayashi, R., and Kamiyama, S., "Effect of Cavitation on the Accuracy of Herschel-Type Venturi Tubes," ASME Paper No. 61-WA-99.

BIF 1405 Home Avenue, Akron, Ohio
Phone 330-564-0941 Fax 330-633-6362
www.bifwater.com Info@bifwater.com

BIF®

Metering Flow... Naturally!